Theory and Technology in Natural Sciences and Watershed Management

Earth Systems Institute

A Topographic Fire Model

Documentation of ESI's Landscape Simulator

A Topographic Fire Model

Fire Model 1
Why we need a fire model. 1
Why we want a new fire model 1
Data to drive such a model 1
Fire occurrence as a function of position relative to local relief 2
Fire occurrence as a function of slope aspect 2
Wind 2
Forest Age 3
Fire Recurrence 3
Fire Shape 3
Ignition Frequency 4
Fire Size 4
References 4

Table 1. Model Parameters 5

Figure 1. Stand-age classes from 1939 aerial photographs. 6
Figure 2. Position relative to local relief. 7
Figure 3. Fire recurrence relative to local relief. 8
Figure 4. Fire recurrence as a function of slope aspect. 9
Figure 5. Topographic variability in fire recurrence. 10
Figure 6. The effect of slope gradient on fire shape. 11
Figure 7. Fire Shapes. 12

Fire Model

Why we need a fire model.

The task is to simulate a continuous time series of sediment flux (and its spatial distribution) in a basin. Mass wasting of shallow soils forms a periodically significant proportion of the sediment flux in certain landscapes. The stability of shallow soils is governed in part by the effective cohesion provided by tree roots. The loss of root strength following forest mortality reduces stability of shallow soils. We thus anticipate an increased probability of shallow mass wasting in those areas where the forest is killed by fire; an increase that will persist until new trees have grown sufficiently to re-established the previous level of root strength. Benda and Dunne (1997) used this reasoning to simulate sediment production from landsliding of shallow soils from hollows in the Oregon Coast range where, prior to timber harvest, lightning-ignited fires comprised the predominant factor in forest mortality. Landslide occurrence was estimated as a function of surface topography, effective soil strength (which via root strength is a function of forest age), and precipitation (via simulated storm intensities and durations). They found that predicted increases in sediment flux in those areas affected by wildfire can create a dramatic short-term increase in the rate of sediment delivery to stream channels through a portion of the channel network. Movement of this a sediment through a downstream point in the network can temporally alter channel characteristics, with an impact that varies with position in the network, and may create terraces. Fires can thus have a controlling impact on long-term channel and riparian environments and on temporal variations in channel and riparian characteristics. In landscapes where these processes are active, prediction of these effects requires prediction of fire occurrence.

Why we want a new fire model

Benda and Dunne (1997) generated forest fires of a size and periodicity appropriate to produce a forest-stand-age distribution similar to that observed for pristine areas, with fire size based on a negative exponential distribution. Ignition points were chosen randomly; the probability of ignition was a function of forest age. Fire shape was roughly circular, with randomly placed unburned islands. This approach produced an appropriate stand-age distribution. That model produced fires without reference to the surface topography. However, surface topography and position in the landscape have great influence on fire location. Because we are interested in the spatial distribution of sediment sources, we want to include all spatial controls on fire occurrence. We have attempted, therefore, to produce a model to predict fire occurrence with reference to pertinent topographic parameters.

Data to drive such a model

We know empirically that fire tends to spread faster upslope than downslope and that fuel availability and combustibility vary with position. How does this affect the position and shape of burned areas? Lacking actual fire scars to examine, we have used a stand-age map for the study area to seek correlations between the probability of burning and certain topographic parameters. The stand-age map is reproduced in Figure 1. Tree age was estimated from 1:12,000-scale areal photographs from 1939 for those areas thought to be unaffected by prior logging. Four age classes were mapped: 0 - 50 years, 50 - 100 years, 100 - 200 years, and greater than 200 years. The mapping was done by a person experienced in examining aerial photographs, but with little forestry expertise, and checked by an experienced forester. Age interpretations were checked by counting

rings in stumps from harvest units of known age. Using a raster GIS, age-class distributions were then determined for different parts of the landscape.

Fire occurrence as a function of position relative to local relief

With a DEM (digital elevation model), each pixel is classified according to its position relative to the local relief. This classification is determined as follows:

- For each pixel, all neighboring pixels within a specified radius (1.8 km for this case) were examined to determine *Zmax* and *Zmin*, the maximum and minimum elevations.
- Each pixel is then classified using the equation

$$R = \frac{Z - Zmin}{Zmax - Zmin}$$

where Z is the elevation of the pixel.

R varies in value from 0 to 1: a value of 0 indicates a position on the valley bottom; a value of 1 indicates a position on the ridge top; intermediate values indicate position on the slope. In Figure 2 topography is shown by the shaded relief image; R values are indicated in the image below with valley bottoms ($R = 0$) indicated by black and ridge tops ($R = 1$) indicated by white.

With this representation, the landscape can be categorized into classes based on position relative to local relief. The bar graph in Figure 3 shows the relative proportion of all areas with a mapped stand age falling into each of 10 classes for R (areas affected by timber harvest were excluded from the analysis). The distribution of stand ages for pixels within each relief class can then be fit with a negative exponential distribution (Van Wagner, 1978) to estimate the fire-recurrence interval for each R class. Results, normalized by area, are shown in the lower two graphs in Figure 3. We find that the probability of burning increase as one moves toward the ridge top, with a corresponding decrease in the fire-recurrence interval. Recurrence intervals vary from a maximum of greater than 800 years in the valley bottoms to a minimum of near 300 years along the ridge tops. The mean recurrence interval overall is 460 years. Using the regression shown in Figure 3 and the map in Figure 2, all points in the landscape can be assigned a probability of burning based on their position relative to local relief.

Fire occurrence as a function of slope aspect

The study area was divided into 30-degree classes based on slope aspect. The proportion of area falling within each class is shown by the bar graph in Figure 4. Using the procedure described above, fire-recurrence intervals were calculated for each class. Results, normalized for area, are shown in the lower graphs in Figure 4. The probability of burning is greatest on slopes having a southwest aspect and lowest on slopes having a north aspect. This relationship likely reflects variations in fuel-moisture content associated with variations in insolation. Using the regression shown in Figure 4, all points in the landscape can be assigned a probability of burning based on aspect.

Wind

The data indicate clear correlations between fire-recurrence interval and position relative to the local relief and slope aspect. We also know that wind has a large influence on fire. I am not sure, however, how to parameterize the landscape so that relationships between wind-driven fire and topography can be recognized. Such a relationship may be revealed by examining fire-recurrence

interval as a function of valley trend, but the correlation with slope aspect confounds any trends detected. I am open to suggestions.

Forest Age

The model currently includes no relationship between forest age and probability of burning, as did Benda and Dunne (1997) and Wimberly and Spies (2000). Such a relationship can be readily included if there is data to indicate it should be.

Fire Recurrence

A fire-recurrence interval based on aspect and position relative to local relief is calculated as the product of the probabilities of burning as functions of relief and aspect (given by the regressions in Figures 3 and 4) normalized to produce the mean recurrence interval of 280 years estimated for this region. The result is shown in Figure 5. Recurrence intervals vary from a less than 200 years on certain southwest-facing ridgetops to more than 400 years in certain north-facing valley bottoms.

The mean recurrence interval applied in this case is 280 years. This is considerably shorter than the 460 years estimated from the stand-age maps based on 1939 aerial photography over about 500 square kilometers. As we will demonstrate, there may be large variability in the recurrence interval of stand-resetting fires, and the magnitude of that variability is a function of the area examined, with larger variability associated with smaller spatial extent. Using regional stand age maps compiled bye Andrews and Cowlin (1934, 1940), involving an area more than 1000 times larger than that examined here, Fahnestock and Agee (1983) estimated a recurrence interval of 220 years and Booth (1991), using the same data, estimated a recurrence interval of 340 years. Our value of 280 years falls midway between these two estimates.

Fire Shape

Fire shape is determined on the basis of an estimated probability of burning calculated for each pixel. Fires spread faster upslope than down, explaining in part the increasing probability of burning as one moves upslope towards the ridge top (Figure 3). Likewise, slopes with a southwest aspect are more likely to burn than slopes with a north aspect (Figure 4). The relative probability of burning for a pixel is thus based on its elevation relative to neighboring pixels and its aspect. This probability is used to calculate a relative fire-spread velocity. In the model, a fire grows from the point of ignition. The rate of spread from pixel to pixel is a function of the relative probability of burning for each pixel. Relative probability (P) is estimated with the product of the probability based on slope gradient (p_s) and the probability based on slope aspect (p_a):

$$P = p_s * p_a.$$

A value for p_a is taken from the regression shown in Figure 4. A value for p_s is based on the rule of thumb given by Chandler et al. (1983): rate of spread doubles for every 10-degree increase in slope. This is represented as

$$p_s = 2^{(S/10)}$$

where S is the slope in degrees from the pixel center that has burned to a neighboring pixel center that has not. Any other characteristic that affects the probability of burning and that can be parameterized within a raster-based representation of spatial location can be incorporated into the rela-

tive probability value for a pixel.

The relative probability of burning for a pixel is translated directly into a fire-spread velocity. Relative travel times for the fire line from the point of ignition are then calculated. Contours of relative travel time indicate fire shape. Travel time is calculated pixel by pixel and continue until the fire has obtained the required size. A ray-tracing algorithm is used for calculating travel times. To illustrate, the effect of slope on fire shape is shown in Figures 6.

Together slope and aspect can be used to estimate fire shape from a given ignition location for the study area. Simulated fires of small size will tend to be isolated to upper slopes and spread along ridges. Simulated large fires will tend to overwhelm local topography and burn across valleys. An example is shown in Figure 7. The polygons represent successively larger fires from a common ignition point. The largest polygon encompasses over 100 km^2.

Ignition frequency

Ignition probability is estimated as a function of regional climatic parameters (Agee and Flewelling, 1983) and is specified in terms of probability per DEM pixel per year. The model currently has no topographic influence on ignition; all points in the landscape are given equal probability. To specify ignition locations for any year, we go through the DEM cell by cell, and for each cell sample a random number from a uniform distribution. If the number obtained is less than the ignition probability, the cell is considered an ignition point. There is thus equal probability of fire from year to year, both for an individual cell and for the study area as a whole, but the stochastic nature of the sampling results in no fires some years and multiple fires other years.

Fire size

Teensma (1987) found for the western Cascade's of Oregon that fire sizes may be represented as a negative exponential distribution: lots of small fires and a few big ones. If we assume that naturally occurring fire sizes in the western Cascades of southern Washington also follow a negative exponential distribution, that distribution is completely determined by the average recurrence interval of fires and the ignition frequency. Thus given the ignition frequency as a function of regional climate, the distribution of fire sizes is completely constrained by the mean fire recurrence interval. We obtain a mean fire size of 22 square kilometers.

References

Agee, J. K., and R. Flewelling, 1983. A fire cycle model based on climate for the Olympic Mountains, Washington. *Seventh Conference on Fire and Forest Meteorology*, Boston, American Meteorology Society: pp. 32-37.

Andrews, H. J. and R. W. Cowlin, 1934. *Forest resources of the Douglas-fir region*. US Dept. of Agriculture, Misc. Pub. 389, 169 p.

Benda, L. E., and T. Dunne, 1997. Stochastic forcing of sediment supply to the channel network from landsliding and debris flow, *Water Resources Research*, vol. 33: 2849-2863.

Chandler, C., P. Cheney, P. Thomas, L. Trabaud, and D. Williams, 1983. *Fire in Forestry*, 2 vols, John Wiley and Sons, New York.

Fahnestock, G. R. and J. R. Agee, 1983. Biomass consumption and smoke production by prehis-

toric and modern forest fires in western Washington, J*ournal of Forestry*, vol. 81: 653-657.

Teensma, P. D. A., 1987. *Fire History and Fire Regimes of the Central Western Cascades of Oregon*, Ph.D. Dissertation, University of Oregon, Eugene, 188 pg.

Van Wagner, C. E., 1978. Age-class distribution and the forest fire cycle, *Canadian Journal of Forest Resources*, vol. 8: 220-227.

Wimberly, M. C., T. A. Spies, C. J. Long, and C. Whitlock, 2000. Simulating Historical Variability in the Amount of Old Forests in the Oregon Coast Range. *Conservation Biology,* vol. 14: 167-180.

Table 1:

Model Parameters	
Mean Recurrence Interval	280 Years
Mean Fire Size (negative exponential distribution)	22 km^2
Ignition Probability	0.00017 ignitions per km^2 per year

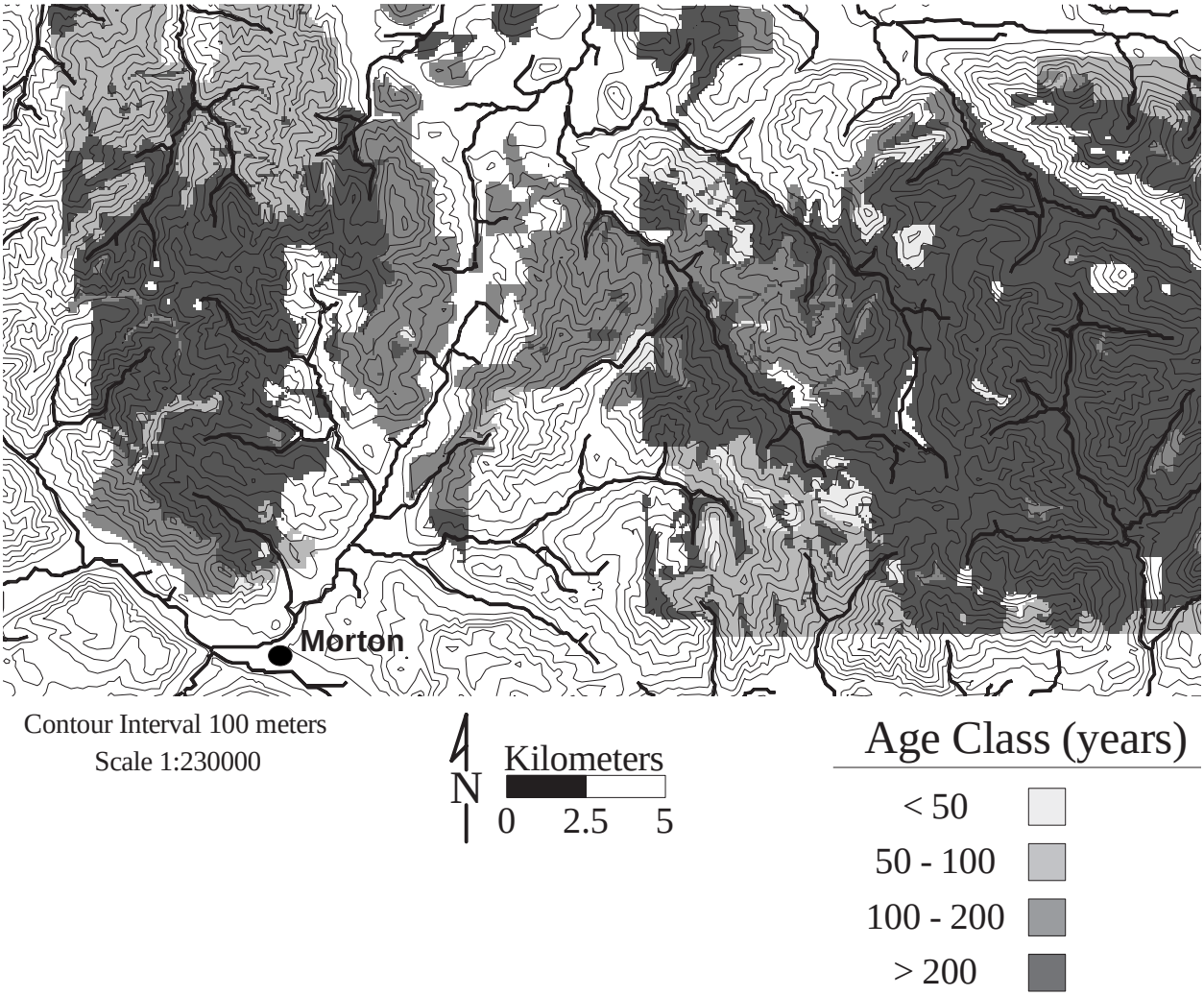

Figure 1. Stand-age classes from 1939 aerial photographs.

White indicates areas not included in the analysis, either because of lack of photography or because of prior logging. The area of mapped stands ages is 500 square kilometers.

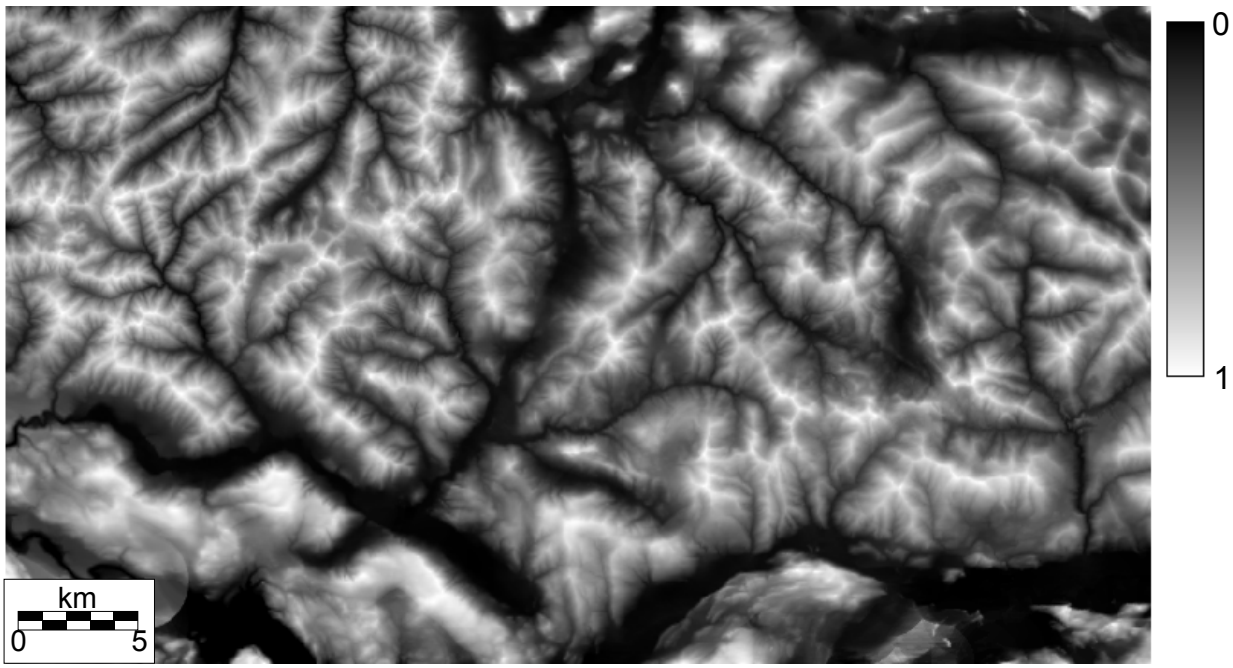

Figure 2. Position relative to local relief.

A value of zero (black) corresponds to a valley floor, a value of 1 (white) corresponds to a ridge top, both relative to a radius of 1.8 kilometers.

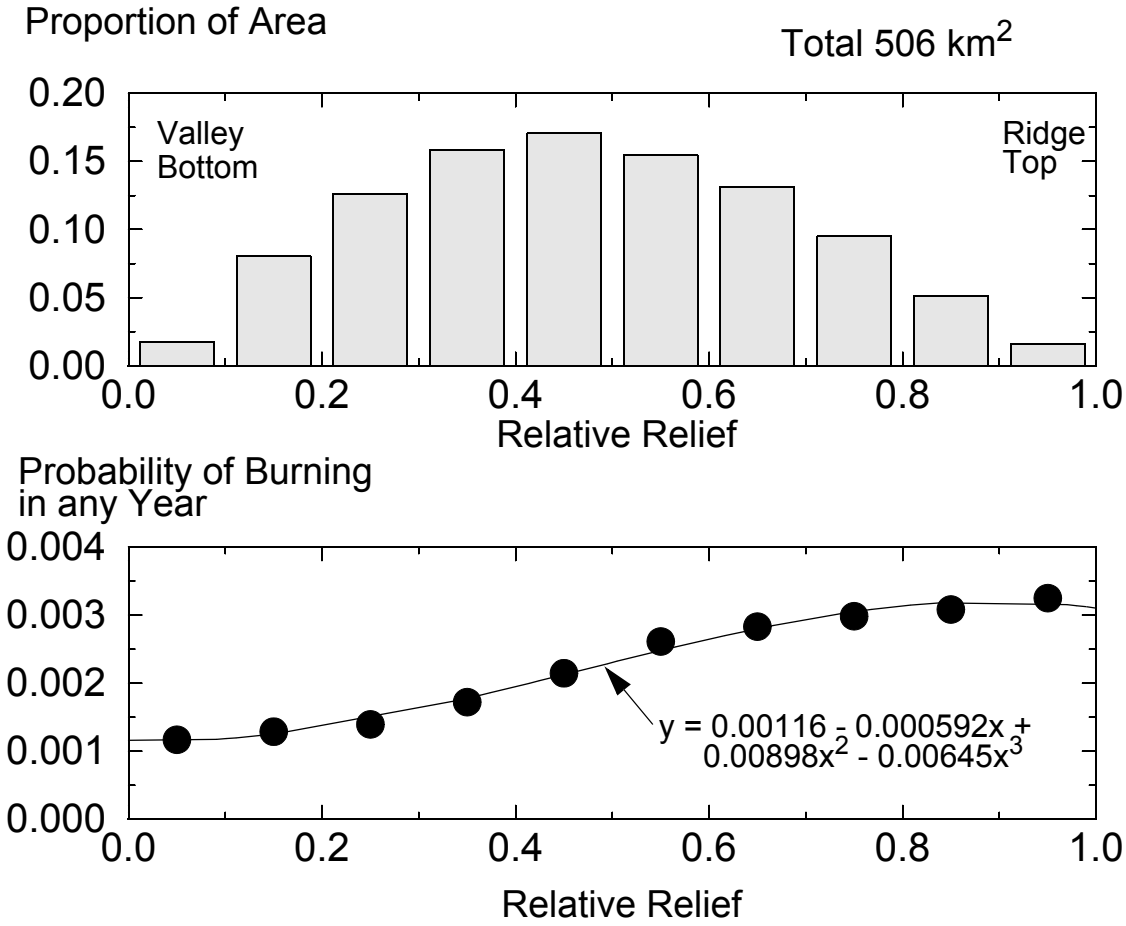

Figure 3. Fire recurrence relative to local relief.

The bar graph at top shows the proportion of the mapped area falling into each of 10 relief classes. The bottom graph shows the probability of burning in any year based on the stand-age distribution found within each relief class. The topographic distribution of stand ages shows that the probability of burning increases from valley floor to ridge top.

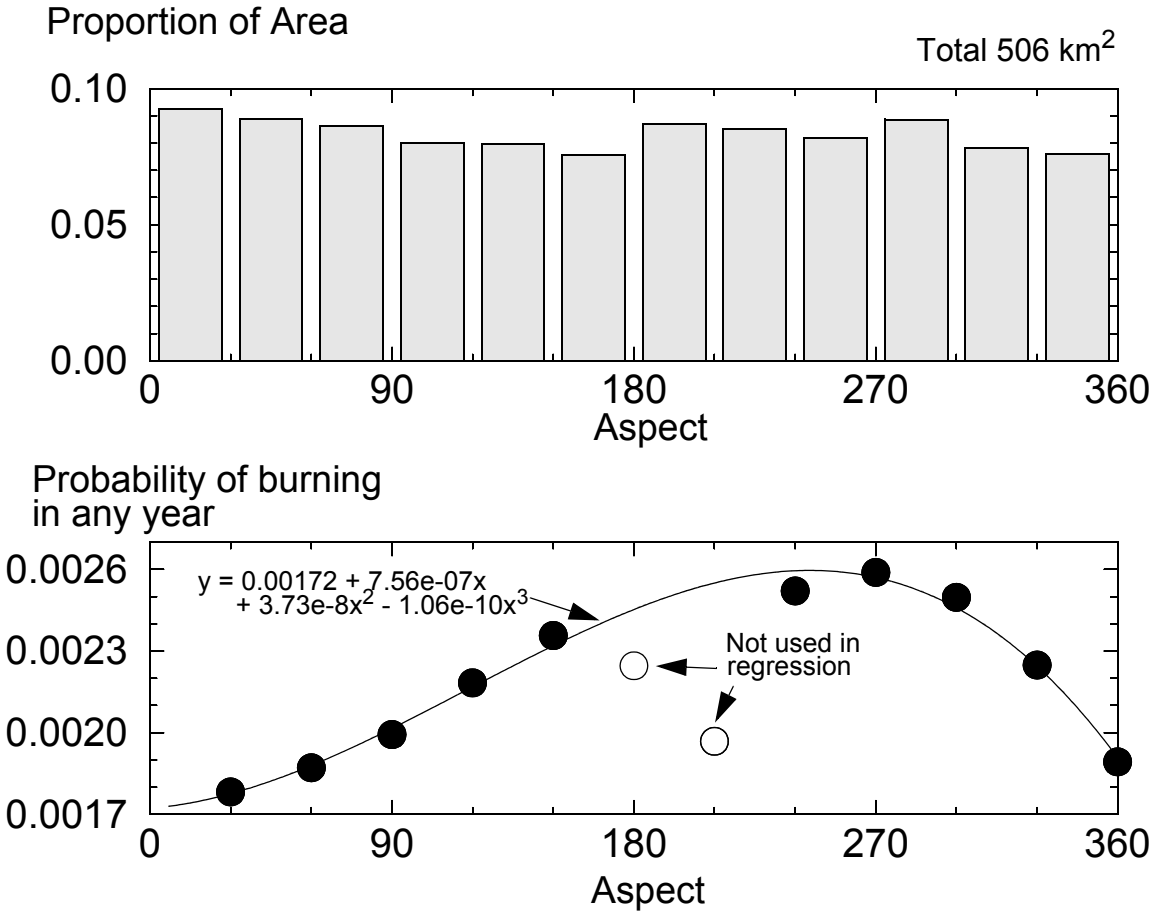

Figure 4. Fire recurrence as a function of slope aspect.

The bar graph shows the proportion of mapped area falling within each 30-degree aspect class. The bottom graph shows the probability of burning for any year based on the stand-age distribution found within each of these aspects. South-west facing slopes have the greatest probability of burning, north facing slopes the least.

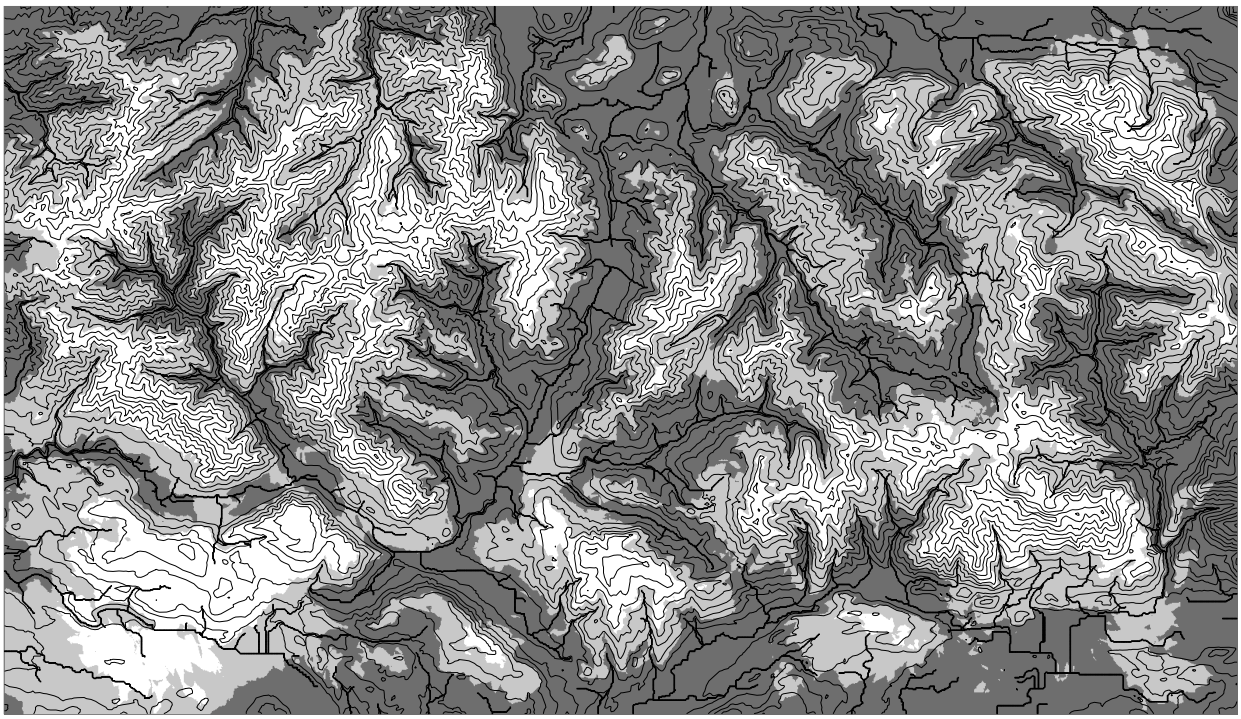

Figure 5. Topographic variability in fire recurrence.

Estimated from one 3000-year fire simulation. Recurrence intervals range from less than 200 years on the ridge tops to greater than 400 years in large valley floors. The spatially averaged value is 280 years.

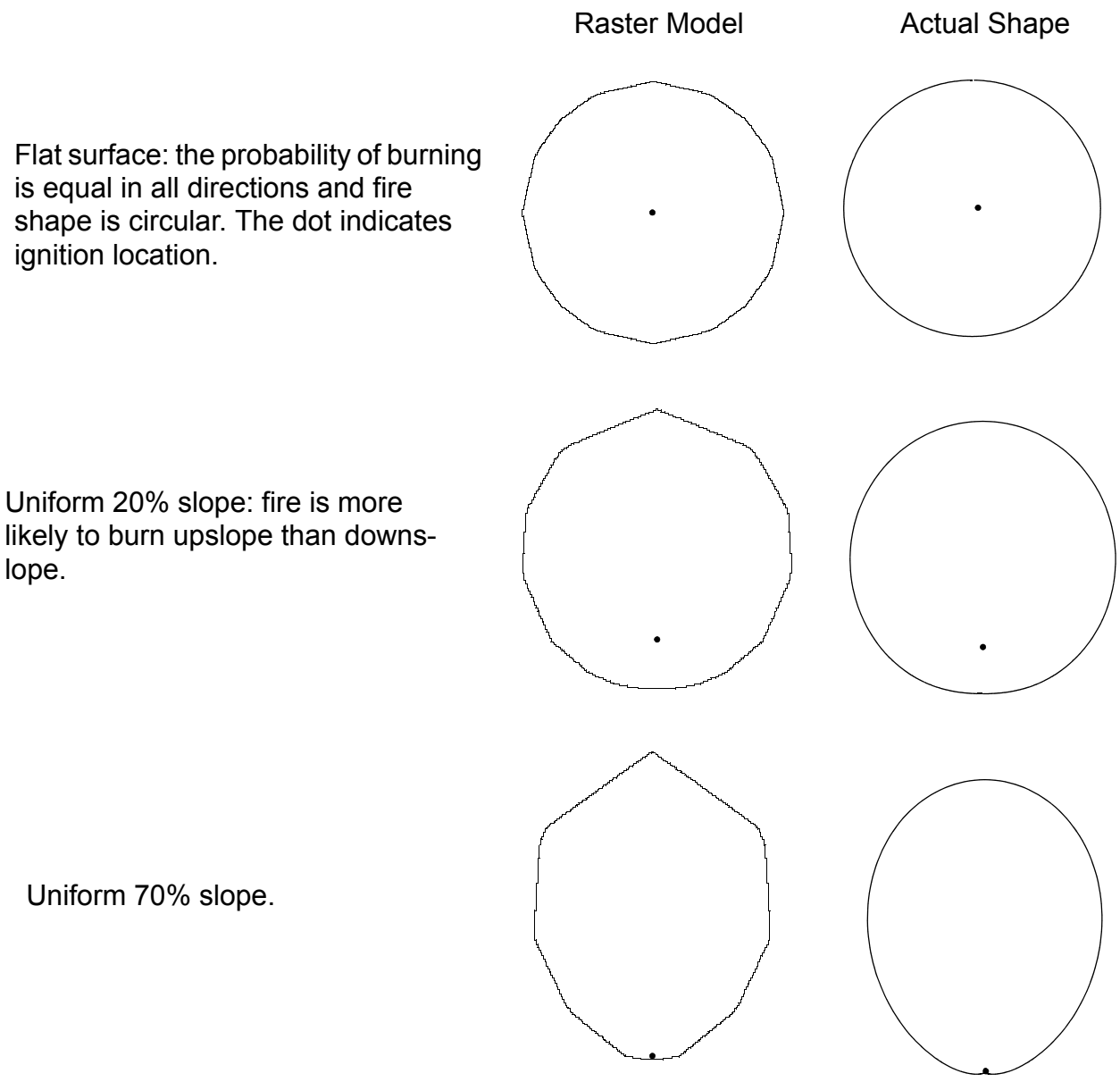

Figure 6. The effect of slope gradient on fire shape.

The fire-shape model accounts for surface slope with the assumption that a fire spreads upslope faster than downslope. For these examples fire-spread velocity is set to double for every 10-degree increase in slope. The shape is estimated by calculating travel times to each grid point in the DEM. A linear interpolation is used for estimating travel times between grid points. A first-order interpolation, as used for these examples, results in rapid processing times, but slightly inaccurate fire shapes. Increased accuracy can be obtained by using a higher-order interpolation scheme - at the cost of increasing processing time. We use a first-order interpolation in our model.

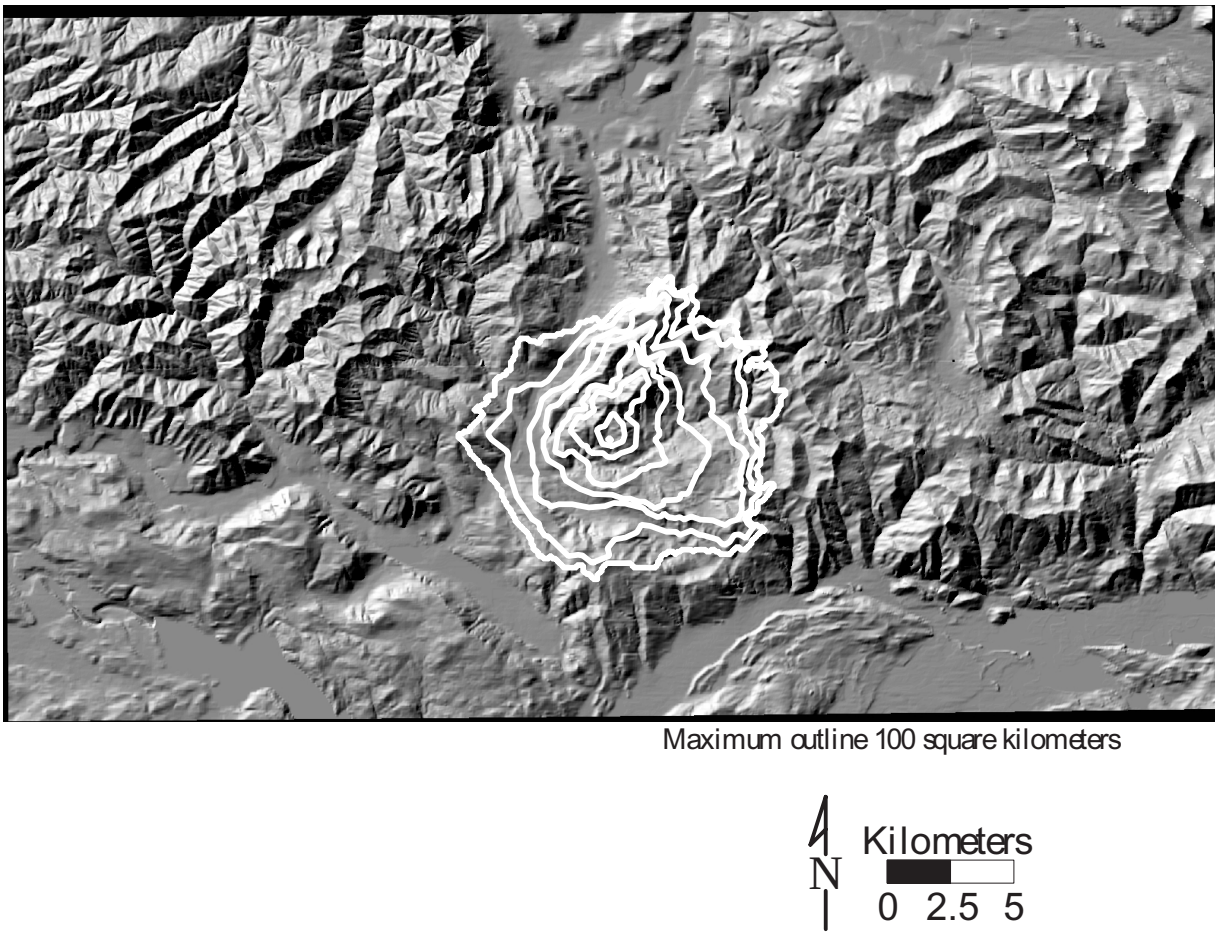

Figure 7. Fire Shapes.

The concentric polygons show simulated fires of increasing size from a common ignition point. Small fires tend to spread upslope and then to grow along ridge tops. Large fires overwhelm the local topography.